JM PAPERS

Transformation of small-amplitude internal waves passing over a bottom step in a two-layer fluid

Susam Boral[1,2] and Yury Stepanyants[3,4],†

[1]College of Shipbuilding Engineering, Harbin Engineering University, Harbin 150001, PR China

[2]Department of Civil, Structural and Environmental Engineering, Trinity College Dublin, Dublin 2, Ireland

[3]School of Mathematics, Physics and Computing, University of Southern Queensland, West St., Toowoomba, QLD 4350, Australia

[4]Department of Applied Mathematics, Nizhny Novgorod State Technical University n.a. R. E. Alekseev, 24 Minin St., Nizhny Novgorod 603950, Russia

The transformation of internal waves on a stepwise underwater obstacle is studied in the linear approximation. The transmission and reflection coefficients are derived for a two-layer fluid. The results are obtained and presented as functions of incident wave wavenumber, density ratio of layers, pycnocline position, and height of the bottom step. Excitation coefficients of evanescent modes are also calculated, and their importance is demonstrated. This allows one to estimate the number of evanescent modes necessary to take into account to attain the required accuracy for the transformation coefficients.

1. Introduction

The more and more intense exploration of oceanic resources in the past decades makes topical the problem of safety and protection of marine engineering constructions, harbours, gulfs, beaches and ships. Great attention has been paid to the consequences of surface wave impacts, especially those caused by tidal and tsunami waves, as well as swells and wind waves. Internal waves represent another typical kind of wave motion in the oceans, and similarly to the surface waves, they commonly occur in the oceans, seas, lakes and other large-scale estuaries, including artificially constructed storage ponds. They can significantly affect climate change, water mixing, migration of plankton, sediment

† Email address for correspondence: yuas50@gmail.com

transport and coastal engineering constructions (platform, oil and gas pipelines, etc.), as well as underwater navigation.

One of the topical problems related to the impact of oceanic waves on the coastal zone is the calculation of wave transformation when waves pass over the continental shelf. This problem has been studied sufficiently well for small-amplitude surface waves passing over the stepwise obstacle. The first entry into the problem was made by Lamb (1932), who derived simple formulae for the transformation coefficients in the long-wave approximation. The rigorous problem statement for quasi-monochromatic linear waves of arbitrary wavelength was considered then by many authors, starting from the seminal paper by Bartholomeusz (1958), who took into account not only travelling waves but also evanescent modes localised in the vicinity of the bottom step edge. The reviews of results obtained can be found, for example, in Massel (1989), Dingemans (1997) and Kurkin, Semin & Stepanyants (2015).

The major outcome of these studies is that exact values of transformation coefficients (the coefficients of transmission and reflection) can be obtained via numerical solution of a set of algebraic equations for the transformation coefficients and coefficients of excitation of evanescent modes. The number of equations required to reach a certain accuracy depends on the depth ratio h_2/h_1, where h_1 is the depth in front of the edge of the bottom step, and h_2 is the depth behind the edge. When the ratio h_2/h_1 is too small (say, of the order of 10^{-2}) or too big (of the order of 10^2), the total number of required equations may reach 500. This is, certainly, not handy for practical applications and theoretical analysis of dependences of the transformation coefficients on the parameters. (In reality, such extreme values of depth drops are out of practical interest.) When a high accuracy is not required, the transmission coefficient can be calculated analytically, taking into consideration only travelling modes and neglecting evanescent modes. This idea was suggested by Miles (1967) and realised in Kurkin *et al.* (2015), where the corresponding analytical formulae were derived. It was shown by comparison with exact formulae and numerical calculations that the transmission coefficient within such approximations can be obtained with an error less than 5 %, whereas the error of the reflection coefficient is much greater (however, the reflection coefficient is usually not so topical from the practical point of view).

Another heuristic approach was suggested by one of these authors for the approximate calculation of transformation coefficients (Giniyatullin *et al.* 2014; Churaev, Semin & Stepanyants 2015; Kurkin *et al.* 2015; Meylan & Stepanyants 2024). The idea of this approach is based on the classical Lamb formulae for the transformation coefficients of long surface waves (Lamb 1932) presented in terms of wave speed ratio on both sides of the bottom-step edge c_2/c_1. As shown in the cited papers, very good agreement with the rigorous analytical approach can be achieved if, in the transmission coefficient, the ratio of group speeds c_{g2}/c_{g1} is used instead of c_2/c_1, whereas in the reflection coefficient, the ratio of phase speeds c_{p2}/c_{p1} is used. This approach has been validated by direct numerical modelling, and it was shown that it is accurate enough, robust, and handy for analysis and application.

The problem of internal wave transformation on a bottom step has not been studied thus far with the same completeness as for surface waves. The transformation coefficients for internal waves passing over the bottom step in a two-layer fluid were derived only in the shallow-water limit, assuming that the density difference between the layers is small, i.e. in the Boussinesq approximation (Brekhovskikh & Goncharov 1994; Miropol'sky 2001; Grimshaw, Pelinovsky & Talipova 2008). On the basis of the derived formula, the problem of internal soliton transformation on the bottom step was studied for different polarities of solitons and position of the pycnocline (sharp density interface between the layers)
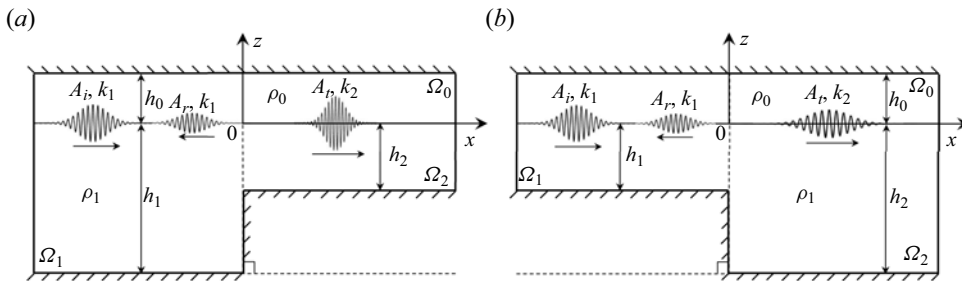
(*a*)

Figure 1. Sketch of the problem geometry: (*a*) $h_2/h_1 < 1$, a wavetrain propagates from the deeper region to the shallower one; (*b*) $h_2/h_1 > 1$, a wavetrain propagates from the shallower region to the deeper one.

(Maderich *et al.* 2009, 2010). For the calculation of transformation coefficients of internal waves of arbitrary wavelength in a two-layer fluid of arbitrary layer densities, only the approximate approach was suggested thus far (Churaev *et al.* 2015). It was demonstrated that the approximate formulae agree well with the numerical data, and can be used for practical applications when high accuracy is not required. However, to our best knowledge, the rigorous approach to the problem of internal wave transformation on a bottom step has not been developed thus far. In this paper, we derive transformation coefficients for linear internal waves in two-layer fluid free from the restriction on wavelength and layer densities. We show that accurate results can be obtained from the solution of an infinite set of algebraic equations for the transformation coefficients of travelling waves and coefficients of excitation of evanescent modes. In practice, the set should be truncated and solved numerically. The number of used equations depends on the required accuracy and hydrological parameters (depth ratio h_2/h_1, density ratio ρ_2/ρ_1, pycnocline depth h_0, dimensionless wavenumber of an incident wave $\kappa = kh_1$). In the limiting case $\rho_2/\rho_1 \to 0$, our results reduce to that for surface waves (see e.g. Massel 1989; Kurkin *et al.* 2015). In another limiting case, $\rho_2/\rho_1 \to 1$ and $\kappa \to 0$, our results reduce to the Lamb-type formulae derived in Grimshaw *et al.* (2008). We show also that the results derived earlier on the basis of the heuristic approach agree well with the rigorous approach developed here. Data from direct numerical modelling also validate our theoretical results. We also derive the relationship between the transmission and reflection coefficients that constitute the energy flux conservation, and show that the theoretical and numerical data agree well with this law.

2. Problem formulation

In this section, we formulate the mathematical model, which we employ to describe the transformation of small-amplitude internal gravity waves passing over the underwater obstacle in the form of a bottom step in a two-layer density stratified fluid. The physical model is considered in a two-dimensional Cartesian coordinate system with x-axis along the mean water level at the interface, and z-axis directed vertically upwards, as exhibited in figure 1. Further, figure 1 illustrates two potential configurations with an incident wave originating either from the deeper region (as seen in figure 1a) or from the shallower region (as depicted in figure 1b). It is assumed that the interface is at the depth h_0 from the water surface, whereas the depth of the rigid bottom bed is $h_j, j = 1, 2$ on either side of the bottom step located at $x = 0$.

We implement the 'rigid lid approximation' at the free surface to effectively filter surface waves (see e.g. Miropol'sky 2001). The fluid is assumed to be inviscid and incompressible,

and flow is considered to be irrotational. Additionally, the densities of the upper and lower layers are assumed to be ρ_1 and ρ_2, respectively, with $a = \rho_1/\rho_2 \leq 1$. Consequently, the velocity potentials exist on both sides of the bottom step, which are introduced as $\boldsymbol{v}_1 = \boldsymbol{\nabla}\varphi_1$ in the domain Ω_1 (see figure 1), and $\boldsymbol{v}_2 = \boldsymbol{\nabla}\varphi_2$ in the domain Ω_2. The velocity potentials satisfy the Laplace equation as the governing equation, and are given by

$$\nabla^2 \phi_i = 0, \quad i = 1, 2. \tag{2.1}$$

The rigid lid approximation at the air–water interface and the impermeable rigid bottom bed boundary conditions yield

$$\frac{\partial \phi_j}{\partial z} = 0 \quad \text{on } z = h_0, \tag{2.2}$$

$$\frac{\partial \phi_j}{\partial z} = 0 \quad \text{on } z = -h_j \text{ for } j = 1, 2. \tag{2.3}$$

Further, the linearised continuity conditions for the fluid velocity and pressure along the interface are presented as (Lamb 1932)

$$\left.\begin{aligned}
\frac{\partial \eta}{\partial t} &= \frac{\partial \phi_i}{\partial z}\bigg|_{z=0^-} = \frac{\partial \phi_i}{\partial z}\bigg|_{z=0^+}, \\
a\left(g\frac{\partial \phi_i}{\partial z} + \frac{\partial^2 \phi_i}{\partial t^2}\right)\bigg|_{z=0^-} &= \left(g\frac{\partial \phi_i}{\partial z} + \frac{\partial^2 \phi_i}{\partial t^2}\right)\bigg|_{z=0^+},
\end{aligned}\right\} \quad \text{for } i = 1, 2, \tag{2.4}$$

where g is the acceleration due to gravity. Then the continuity of pressure and velocity along the step wall at $x = 0$ gives

$$h_1 > h_2 \quad \begin{cases} \phi_1(0, z) = \phi_2(0, z) & \text{for } -h_2 < z < h_0, \\ \phi_{1x}(0, z) = \phi_{2x}(0, z)H(z + h_2) & \text{for } -h_1 < z < h_0, \end{cases} \tag{2.5}$$

$$h_1 < h_2 \quad \begin{cases} \phi_1(0, z) = \phi_2(0, z) & \text{for } -h_1 < z < h_0, \\ \phi_{1x}(0, z)H(z + h_1) = \phi_{2x}(0, z) & \text{for } -h_2 < z < h_0, \end{cases} \tag{2.6}$$

where H is the Heaviside unit step function.

As we study the scattering problem, we assume that in the far-field zone, $|x| \to \infty$, the boundary conditions are

$$\phi_1 = A_i \exp(\mathrm{i}(k_{10}x - \omega t)) + A_{r0}\exp(-\mathrm{i}(k_{10}x - \omega t)) \quad \text{as } x \to -\infty, \tag{2.7}$$

$$\phi_2 = A_{t0}\exp(\mathrm{i}(k_{20}x - \omega t)) \quad \text{as } x \to \infty, \tag{2.8}$$

where k_{j0} for $j = 1, 2$ are wavenumbers of plane progressive waves in the reflection and transmission zones.

3. Plane wave solution

Let us consider a plane wave travelling on the pycnocline between two layers in a fluid of finite depth. In the linear approximation, the interfacial wave can be presented as

$\eta = A \exp(\mathrm{i}(kx - \omega t))$. The associated velocity potential can be presented in each layer in the form (Brekhovskikh & Goncharov 1994)

$$\phi = \begin{cases} -\mathrm{i}\dfrac{A\omega}{k}\dfrac{\cosh k(z - h_0)}{\sinh kh_0}\exp(\mathrm{i}(kx - \omega t)) & \text{for } -\infty < x < \infty,\, 0 < z < h_0, \\[4mm] \mathrm{i}\dfrac{A\omega}{k}\dfrac{\cosh k(z + h_j)}{\sinh kh_j}\exp(\mathrm{i}(kx - \omega t)) & \text{for } -\infty < x < \infty,\, -h_j < z < 0, \end{cases} \tag{3.1}$$

where the wave frequency ω is linked with the wavenumber k_j by the dispersion relation

$$\omega^2 = \frac{(1 - a)gk_j}{a \coth k_j h_0 + \coth k_j h_j}. \tag{3.2}$$

This dispersion relation reduces to the dispersion relation for surface gravity waves if $a = 0$. It is worth mentioning that the dispersion relation (3.2) possesses one positive real root that pertains to the travelling mode, and an infinite number of purely imaginary roots that pertain to evanescent modes, in each region Ω_1 and Ω_2 shown in figure 1. For such modes, the dispersion relation follows from (3.2) by replacing k_j with $\mathrm{i}\gamma_j$; then it takes the form

$$\omega^2 = \frac{-(1 - a)g\gamma_j}{a \cot \gamma_j h_0 + \cot \gamma_j h_j}. \tag{3.3}$$

4. Method of solution

In this section, we present a complete solution of internal wave scattering by the bottom step in a two-layer fluid in terms of the velocity potential. The velocity potentials are considered as sums of travelling and evanescent modes:

$$\phi_1(x, z) = \frac{\mathrm{i}\omega}{k_{10}}\left(A_i \exp(\mathrm{i}k_{10}x) + A_{r0}\exp(-\mathrm{i}k_{10}x)\right)f_{10}(z) + \sum_{n=1}^{\infty}\frac{\omega}{\gamma_{1n}}A_{rn}\exp(\gamma_{1n}x)f_{1n}(z), \tag{4.1}$$

$$\phi_2(x, z) = \frac{\mathrm{i}\omega}{k_{20}}A_{t0}f_{20}(z)\exp(\mathrm{i}k_{20}x) + \sum_{n=1}^{\infty}\frac{\omega}{\gamma_{2n}}A_{tn}\exp(-\gamma_{2n}x)f_{2n}(z), \tag{4.2}$$

where A_{rn} and A_{tn} for $n = 0, 1, 2, \ldots$ are the unknown amplitudes associated with the reflected and transmitted waves, whereas A_i is known incident wave amplitude. The vertical eigenfunctions $f_{j0}(z)$ are given by (cf. (3.1))

$$f_{j0}(z) = \begin{cases} -\dfrac{\cosh k_{j0}(z - h_0)}{\sinh k_{j0}h_0} & \text{for } 0 \le z < h_0, \\[4mm] \dfrac{\cosh k_{j0}(z + h_j)}{\sinh k_{j0}h_j} & \text{for } -h_j < z < 0, \end{cases} \tag{4.3}$$

for $j = 1, 2$. The vertical eigenfunctions f_{jn} for $n = 1, 2, 3, \ldots$ can be obtained similarly by replacing the wavenumber k_{jn} with $\mathrm{i}\gamma_{jn}$. Substituting (4.1) and (4.2) in (2.5), we get

$$
\begin{cases}
\dfrac{\mathrm{i}}{k_{10}} (1 + R_0) f_{10}(z) + \displaystyle\sum_{n=1}^{\infty} \dfrac{1}{\gamma_{1n}} R_n f_{1n}(z) \\
\quad = \dfrac{\mathrm{i}}{k_{20}} T_0 f_{20}(z) + \displaystyle\sum_{n=1}^{\infty} \dfrac{1}{\gamma_{2n}} T_n f_{2n}(z) & \text{for } -h_2 < z < h_0, \\[2mm]
\mathrm{i}(1 - R_0) f_{10}(z) + \displaystyle\sum_{n=1}^{\infty} R_n f_{1n}(z) \\
\quad = \left\{ \mathrm{i} T_0 f_{20}(z) - \displaystyle\sum_{n=0}^{\infty} T_n f_{2n}(z) \right\} H(z + h_2) & \text{for } -h_1 < z < h_0,
\end{cases}
\tag{4.4}
$$

where $R_n = A_{rn}/A_i$ and $T_n = A_{tn}/A_i$. Similarly, substituting (4.1) and (4.2) in (2.6) yields

$$
\begin{cases}
\dfrac{\mathrm{i}}{k_{10}} (1 + R_0) f_{10}(z) + \displaystyle\sum_{n=1}^{\infty} \dfrac{1}{\gamma_{1n}} R_n f_{1n}(z) \\
\quad = \dfrac{\mathrm{i}}{k_{20}} T_0 f_{20}(z) + \displaystyle\sum_{n=1}^{\infty} \dfrac{1}{\gamma_{2n}} T_n f_{2n}(z) & \text{for } -h_1 < z < h_0, \\[2mm]
\left\{ -(1 - R_0) f_{10}(z) + \displaystyle\sum_{n=1}^{\infty} R_n f_{1n}(z) \right\} H(z + h_1) \\
\quad = -T_0 f_{20}(z) - \displaystyle\sum_{n=0}^{\infty} T_n f_{2n}(z) & \text{for } -h_2 < z < h_0.
\end{cases}
\tag{4.5}
$$

5. Results and discussions

Here, we apply the formulae derived in the previous section to the analysis of transformation coefficients setting the following parameters: $\rho_2 = 1025$ kg m^{-3}, $g = 9.81$ m s^{-2} and $a = 0.9$, unless otherwise mentioned below. The infinite sums in (A11) and (A12) are truncated to contain a finite number of terms, N. A convergence study on transformation coefficients has been made to determine an appropriate number of terms N for the subsequent analysis.

Tables 1–3 show that 400 evanescent modes for $h_2/h_1 < 1$ and 200 evanescent modes for $h_2/h_1 > 1$ are quite sufficient to get five decimal places accuracy in the transformation coefficients, irrespective of the ratio of water depths.

Figure 2 demonstrates the variations of the reflection and transmission coefficients as functions of the water depth ratio h_2/h_1 ($0.01 < h_2/h_1 < 100$) for different values of dimensionless wavenumber $\kappa = kh_1$ with $h_0/h_1 = 0.1$. It shows that a significant amount of wave energy is reflected and transmitted when $h_2/h_1 < 1$. Besides, the transmission coefficient K_t is greater than 1 for certain values of $h_2/h_1 < 1$, irrespective of the values of κ. However, for large values of κ, e.g. for $\kappa = 10$, the transmission coefficient is a non-monotonic function of depth ratio in the range $h_2/h_1 < 1$. This phenomenon has been revealed both for surface (Kurkin *et al.* 2015) and internal (Churaev *et al.* 2015) waves. In figure 2, we present the reflection and transmission coefficients obtained both within the current study and with the help of approximate formulae proposed in Churaev *et al.* (2015)

N	K_r	K_t
50	0.1238896	1.1422038
100	0.1238771	1.1422056
150	0.1238730	1.1422061
200	0.1238710	1.1422064
250	0.1238698	1.1422066
300	0.1238690	1.1422067
350	0.1238689	1.1422067
(a) $h_2/h_1 = 0.1$		

N	K_r	K_t
10	0.0014261	1.0001303
50	0.0014261	1.0001303
100	0.0014261	1.0001303
(b) $h_2/h_1 = 10$		

Table 1. Convergence study for two different values of h_2/h_1 with $\kappa = 1$ and $h_0/h_1 = 0.1$.

N	K_r	K_t
50	0.3177156	1.3004093
100	0.3184318	1.3000798
150	0.3183826	1.3001024
200	0.3183763	1.3001053
250	0.3183638	1.3001111
300	0.3183765	1.3001053
350	0.3183683	1.3001091
400	0.3183663	1.3001100
450	0.3183663	1.3001100
(a) $h_2/h_1 = 0.1$		

N	K_r	K_t
10	0.0507847	1.0216736
50	0.0507847	1.0216736
100	0.0507847	1.0216736
(b) $h_2/h_1 = 10$		

Table 2. Convergence studies for two different values of h_2/h_1 with $\kappa = 1$ and $h_0/h_1 = 1$.

for $a = 0.9961$. Some discrepancies between the data can be explained by the influence of the non-Boussinesq effect in our case with $a = 0.9$.

For $h_2/h_1 > 1$, the reflection coefficient K_r is close to zero, consequently the transmission coefficient is close to unity for $\kappa = 0.1$, 1 and 10.

The importance of evanescent modes in the scattering phenomenon has been mentioned in the literature; their role in the scattering of surface gravity waves in a homogeneous fluid was studied in Kurkin *et al.* (2015). In figure 3, we show excitation coefficients A_{rj}/A_i, for $j = 1, \ldots, 5$, of the first five evanescent wave modes that appear on the left from the bottom step edge for three values of κ as functions of the depth ratio h_2/h_1. Figure 3 reveals that the excitation coefficients, being rather small, attain maxima for certain values of $h_2/h_1 < 1$. The role of higher-order evanescent modes hardly becomes visible regardless of the thickness of the lower layer h_2. Noticeably, the coefficients A_{rj}/A_i,

N	K_r	K_t
50	0.2988206	1.2591978
100	0.2988096	1.2592023
150	0.2988084	1.2592028
200	0.2988079	1.2592030
250	0.2988077	1.2592031
	(a) $h_2/h_1 = 0.1$	

N	K_r	K_t
10	0.0192953	1.0578001
50	0.0208304	1.0577112
100	0.0208869	1.0577088
150	0.0208974	1.0577083
200	0.0209011	1.0577082
250	0.0209028	1.0577081
300	0.0209028	1.0577081
	(b) $h_2/h_1 = 10$	

Table 3. Convergence studies for two different values of h_2/h_1 with $\kappa = 1$ and $h_0/h_1 = 10$.
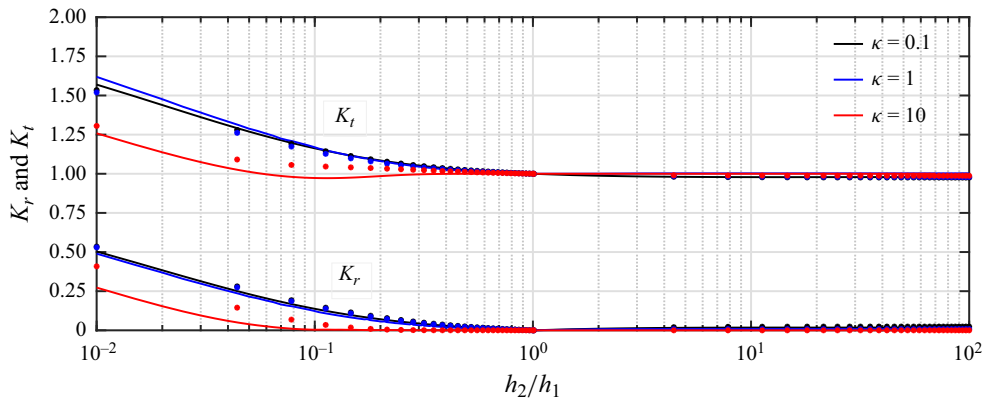
Figure 2. Variations of the reflection coefficient K_r and transmission coefficient K_t for different values of the dimensionless wavenumber κ for $h_0/h_1 = 0.1$ and $a = 0.9$. Colour dots show the results derived with the help of the approximate formulae proposed in Churaev *et al.* (2015) for $a = 0.9961$.

$j = 1, \ldots, 5$, possess multiple zero minima with maxima in the interim for $h_2/h_1 < 1$; then they smoothly approach small constant values when h_2/h_1 becomes greater than 1. As follows from figure 3, the dependence of excitation coefficients A_{rj}/A_i on h_2/h_1 qualitatively is the same for all three values of κ. However, their values at $\kappa = 1$ are much greater than at $\kappa = 0.1$ or at $\kappa = 10$. In all cases, the amplitude of the first evanescent mode A_{r1}/A_i is noticeably greater than amplitudes of other evanescent modes with $j > 1$. This supports Miles' idea (Miles 1967) that the first evanescent mode plays a dominant role, and transformation coefficients can be evaluated with an acceptable accuracy by using only one first evanescent mode in the sums of (A11) and (A12). This idea was realised in Kurkin *et al.* (2015).

Figures 4 and 5, as well as figures 6 and 7, show the same dependences as in figures 2 and 3 but for $h_0/h_1 = 1$ and $h_0/h_1 = 10$, respectively. However, the reflection and transmission
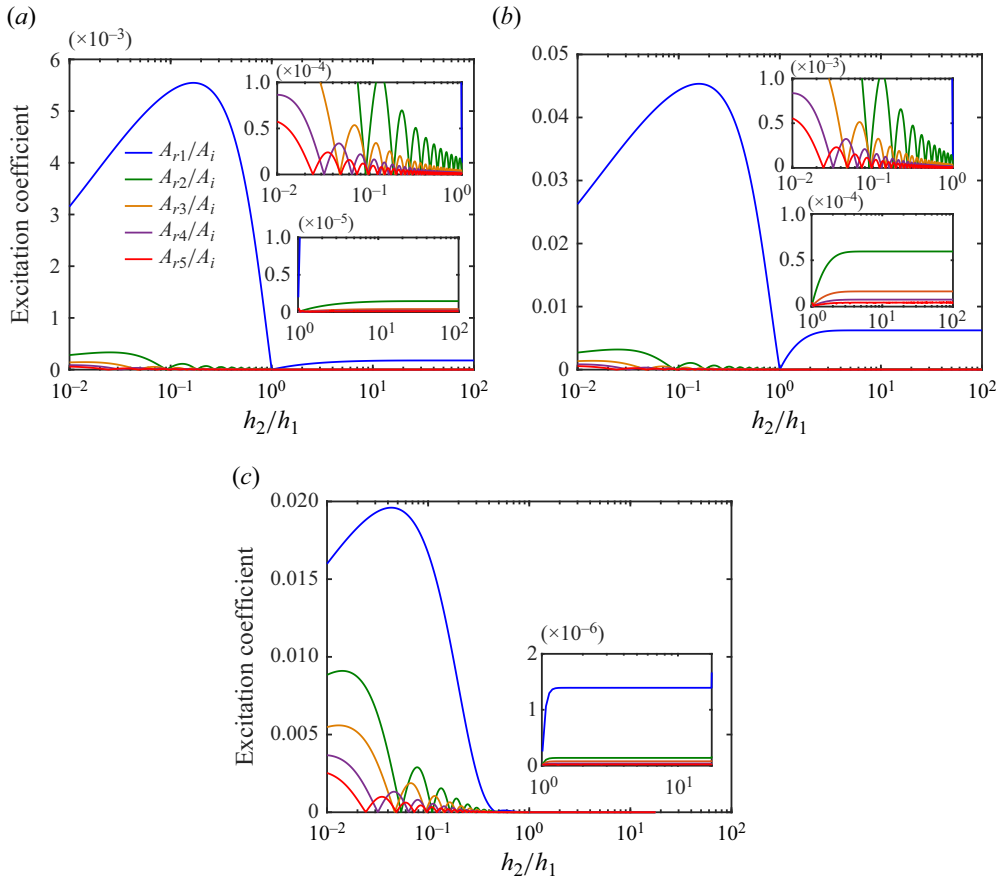
Figure 3. Variations of the first six excitation coefficients associated with the reflected wave amplitudes A_{rj}/A_i, $j = 1, 2, \ldots, 5$, versus depth ratio h_2/h_1 for different values of dimensionless wavenumber κ for $h_0/h_1 = 0.1$: (a) $\kappa = 0.1$, (b) $\kappa = 1$, (c) $\kappa = 10$.

coefficients become greater in the range $h_2/h_1 < 1$ when the ratio h_0/h_1 increases. A simultaneous increase of the reflection and transmission coefficients does not contradict the energy flux conservation because the increase in wave amplitude is accompanied by a decrease in the wavelength.

One can notice that fewer numbers of zero minima and maxima occur for $h_2/h_1 < 1$ when h_0/h_1 increases from 0.1 to 10.

Noticeably, figures 2, 4 and 6 show that practically complete wave transmission occurs when h_2/h_1 becomes greater than unity, regardless of the depth of the interface from the rigid surface h_0. When the pycnocline position becomes closer to the bottom so that h_0/h_1 is too big, and the depth ratio h_2/h_1 is too small, a numerical solution of the systems (A11) and (A12) becomes difficult and even impossible. Apparently, this happens because the main matrix of the system becomes ill-conditioned. In particular, we were unable to obtain a numerical solution for $h_0/h_1 = 10$ when $\kappa = 10$ and $h_2/h_1 < 0.03$ (see figure 6). Apparently, a more advanced asymptotic analysis is needed to get solutions for small and large depth ratios. Note that the approximate formulae derived in Churaev *et al.* (2015) are in good agreement with the analytical formulae developed here for $h_2/h_1 > 1$, irrespective of the pycnocline position and non-dimensional wavenumber.
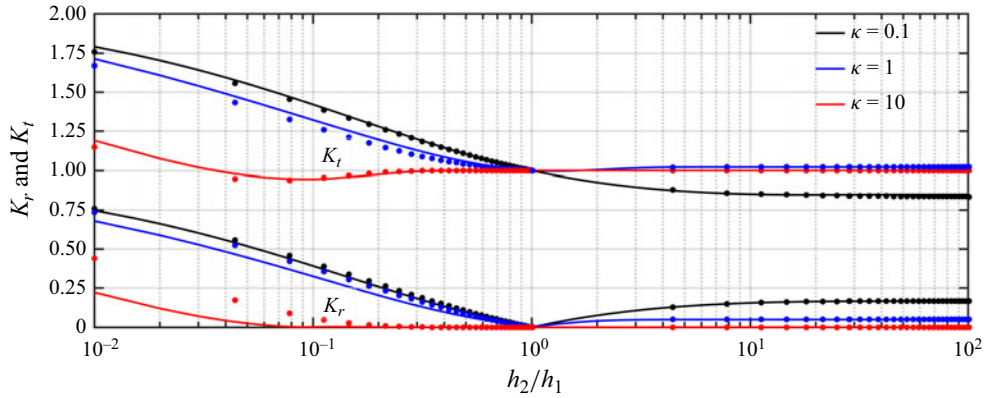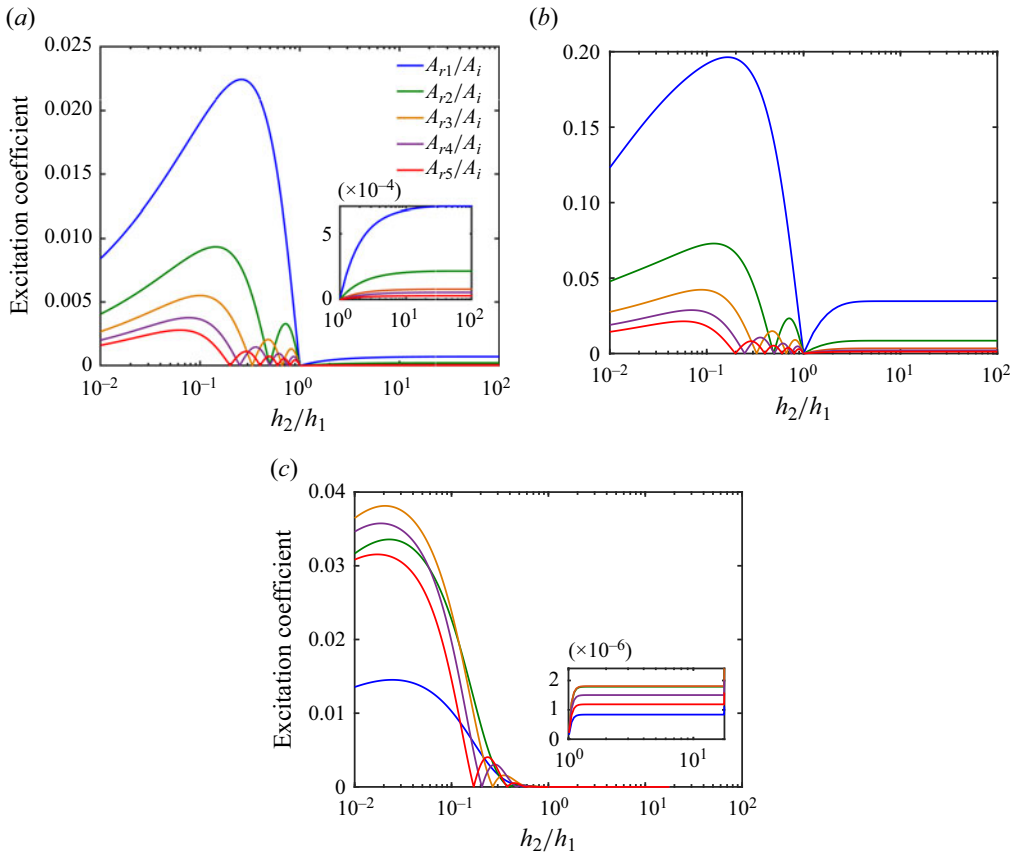
Figure 4. The same as in figure 2 but for $h_0/h_1 = 1$.

Figure 5. The same as in figure 3 but for $h_0/h_1 = 1$: (a) $\kappa = 0.1$, (b) $\kappa = 1$, (c) $\kappa = 10$.

It is interesting to note that while the first evanescent mode with the coefficient A_{r1} predominates in figures 7(a) and 7(b) for $\kappa = 0.1$ and $\kappa = 1$ when $h_2/h_1 < 1$, the second evanescent mode with the coefficient A_{r2} predominates in figure 7(c) for $kh_0 = 10$. Note that for small h_2/h_1, the excitation coefficient of the third mode becomes predominant in
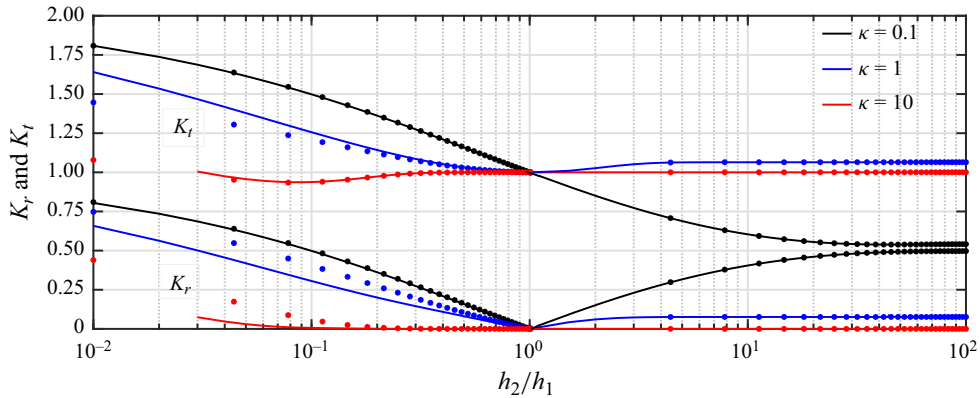
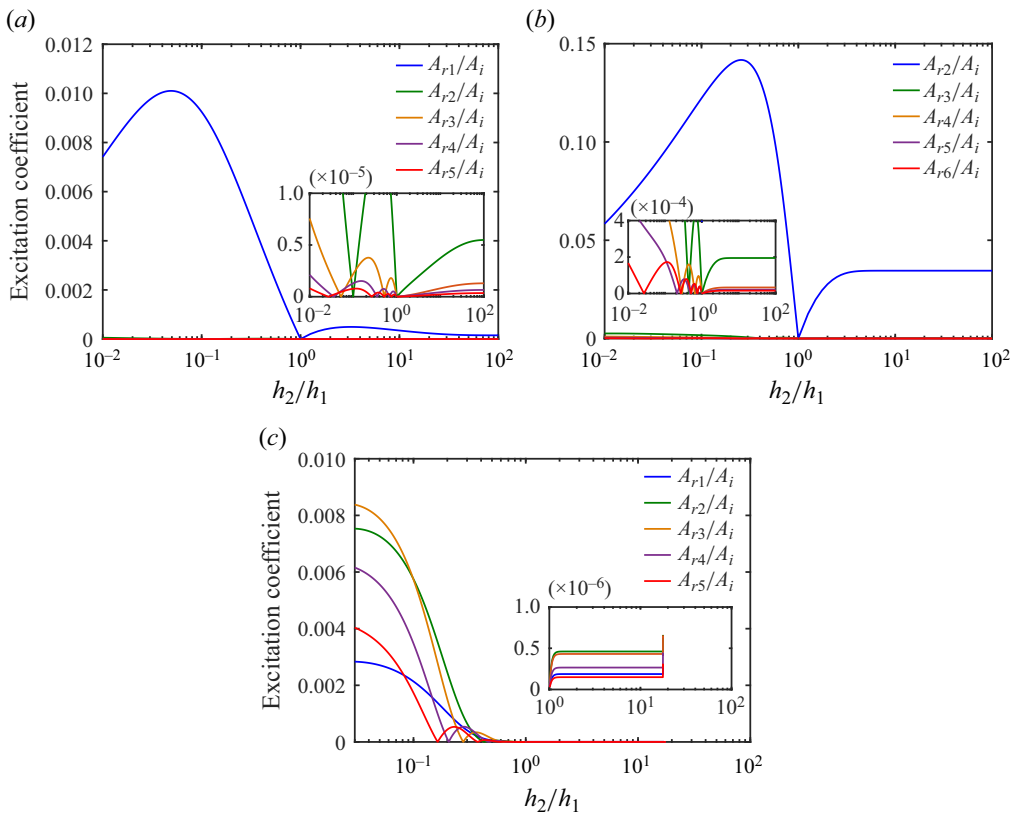Figure 6. The same as in figure 2 but for $h_0/h_1 = 10$.

Figure 7. The same as in figure 3 but for $h_0/h_1 = 10$: (*a*) $\kappa = 0.1$, (*b*) $\kappa = 1$, (*c*) $\kappa = 10$.

the case of deep-water waves shown in figures 5(*c*) and 7(*c*). Figures 3, 5 and 7 provide an estimate of considering a higher number of evanescent modes to obtain the transformation coefficients for a given accuracy. It may be noted that in Churaev *et al.* (2015), the authors studied the transformation problem on the basis of the heuristic formula leaving aside the evanescent modes.
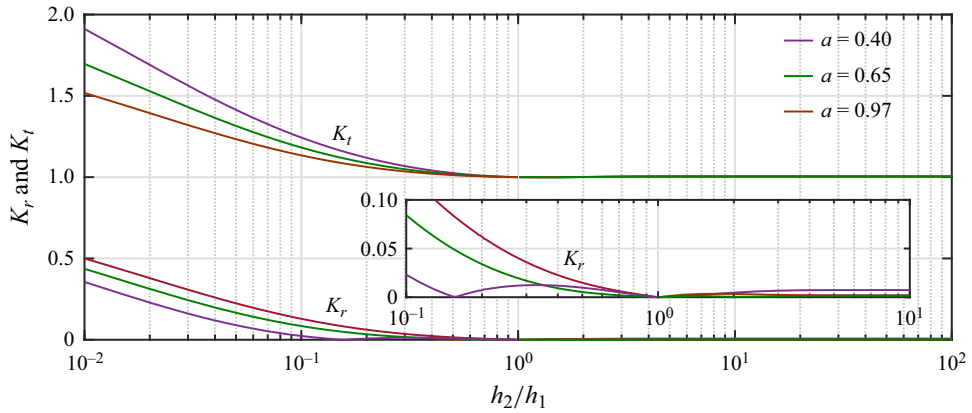
Figure 8. Influence of the density ratio a on transmission coefficients K_r and K_t for $h_0/h_1 = 0.1$ and $\kappa = 1$.
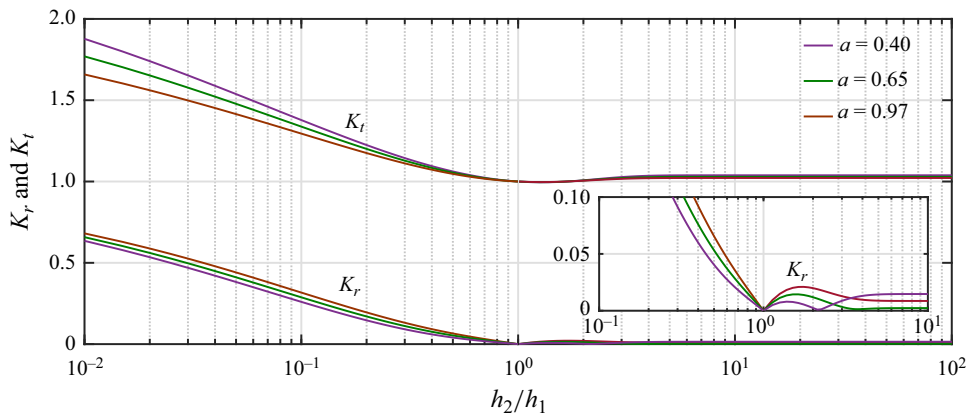

Figure 9. The same as in figure 8 but with $h_0/h_1 = 1$.
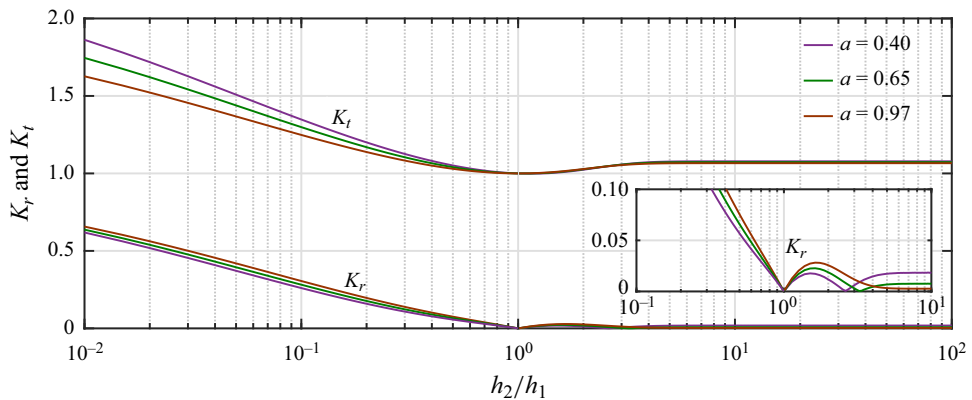
Figure 10. The same as in figure 8 but with $h_0/h_1 = 10$.

Figures 8–10 demonstrate the influence of the density ratio $a = \rho_1/\rho_2$ on the reflection and transmission coefficients for different values of the depth ratio h_0/h_1 with $\kappa = 1$. Qualitatively, the shown dependences are similar: the smaller the parameter a, the bigger the transmission coefficient and the smaller the reflection coefficient. The influence of

this parameter is noticeable only for $h_2/h_1 < 1$. The analysis of these three figures reveals that the reflection coefficient K_r has a minimum that can be zero not only at $h_2/h_1 = 1$. In particular, $K_r = 0$ at $h_2/h_1 \approx 0.15$ in the case $a = 0.4$ (see figure 8). Positions of secondary minima depend on the relative depth of a pycnocline that is characterised by the parameter h_2/h_1; minima of K_r can occur at $h_2/h_1 > 1$ as illustrated by figures 9 and 10.

To conclude this section, we mention that in all calculations presented above, the quantity F defined in (A22) was indistinguishable from 1 up to the numerical accuracy.

6. Concluding remarks

In this paper, we have addressed a gap in the derivation of transformation coefficients for internal waves in a two-layer fluid due to scattering on the underwater step. This study extends earlier known results (Grimshaw *et al.* 2008) for long internal waves in a two-layer fluid. For fluid of arbitrary depth and density ratio, we have derived an infinite set of equations for the transmission and reflection coefficients, as well as for the excitation coefficients of evanescent modes localised on both sides of the bottom step edge. This set of equations was solved numerically after truncation with a finite number N of equations. The number of equations in our calculations attained $N = 450$ (see table 2), but in fact can be much fewer because the amplitudes of evanescent modes quickly decrease with mode number. We presented the analysis of transformation coefficients for the different dimensionless wavenumbers of an incident wave $\kappa = kh_1$, different relative depths of a pycnocline h_0/h_1, and different values of the density ratio $a = \rho_1/\rho_2$. We have derived the relationship between the transmission and reflection coefficients that constitute the energy flux conservation, and show that the theoretical and numerical data agree well with this law; this can be considered as an independent validation of the results obtained. In such fullness, the problem of internal wave transformation on a bottom step has not been studied thus far even in the linear approximation.

The constructed transformation coefficients and their dependences on parameters agree well with earlier obtained results of the direct numerical modelling of internal wave transformation and approximate heuristic formulae (Churaev *et al.* 2015), as well as with the results obtained for surface waves in a homogeneous fluid (Kurkin *et al.* 2015). We have also demonstrated that Miles' idea (Miles 1967) to use only one first evanescent mode to calculate the transformation coefficients analytically can be quite acceptable when high accuracy is not required. However, an important question on the character of amplitude decay of evanescent modes with the mode number remains open; this can be a matter for a separate study.

It is worthwhile mentioning that the derived formulae are free from the Boussinesq approximation and can be used for any density ratio $a = \rho_1/\rho_2$ of fluid layers. Such situations when the Boussinesq approximation becomes inapplicable can be met in some technological processes where fluids of different densities are considered. Other examples can occur in oceans. As is well known, nowadays oil spill accidents rather often occur in oceans leading to the two-layer oil–water fluid with density ratio $\rho_1/\rho_2 \approx$ 0.8–0.9. Another example when the Boussinesq approximation becomes inapplicable is the interface between clean water overlaying a mud layer near the bottom with a big density difference between the layers.

Further development of the results obtained can be associated with the influence of nonlinearity on wave transformation. The nonlinear effects in the internal solitary wave transformation on a bottom step were studied in Grimshaw *et al.* (2008) and Maderich *et al.* (2009, 2010) in the long-wave approximation. It is also a matter of interest to consider

a transformation of internal envelope solitons and breathers on the underwater step similar to what was considered for surface waves (Ducrozet, Slunyaev & Stepanyants 2021).

We have studied here a model problem of wave transformation on the stepwise bottom topography with sharp change of the depth. In the opposite limit when the topography is smooth compared to the wavelength, the traditional WKB approximation can be used. For some particular bottom profiles, exact solutions can be obtained (see e.g. Churilov & Stepanyants (2022*a*,*b*) and references therein).

Author ORCIDs.

Susam Boral https://orcid.org/0000-0003-0590-5442;

Yury Stepanyants https://orcid.org/0000-0003-4546-0310.

Appendix. Numerical determining of the transformation coefficients and coefficients of evanescent mode excitation

Equations (4.4) and (4.5) represent an infinite system of equations with an infinite number of unknowns, which include the reflected and transmitted wave amplitudes R_0 and T_0, respectively, and coefficients of excitation of evanescent modes R_n and T_n for $n \geq 1$. The approach for resolving such systems was outlined initially in the seminal work of Takano (1960), and subsequently adapted to solutions of similar problems (see e.g. Takano 1967; Massel 1989; Dingemans 1997; Kurkin *et al.* 2015; Meylan & Stepanyants 2024). Employing this methodology, we integrate each equation over the vertical coordinate z from the bottom to the rigid lid, incorporating appropriately selected weights from the vertical eigenfunctions denoted as $f_{jn}(z)$.

The methodology proposed by Takano (1960) involves a sequence of orthogonal functions appropriate for the dispersion characteristics of surface gravity waves. However, this framework does not hold for internal gravity waves. Therefore, we integrate the system (2.5) over z with suitably chosen weight functions:

$$h_1 > h_2 \quad \begin{cases} \displaystyle\int_{-h_2}^{h_0} \phi_1(0,z) f_{2m}(z)\,\mathrm{d}z = \int_{-h_2}^{h_0} \phi_2(0,z) f_{2m}(z)\,\mathrm{d}z, \\ \displaystyle\int_{-h_1}^{h_0} \phi_{1x}(0,z) f_{1m}(z)\,\mathrm{d}z = \int_{-h_1}^{h_0} \phi_{2x}(0,z) f_{1m}(z)\, H(z+h_2)\,\mathrm{d}z. \end{cases} \tag{A1}$$

Similarly, we integrate the system (2.6):

$$h_1 < h_2 \quad \begin{cases} \displaystyle\int_{-h_1}^{h_0} \phi_1(0,z) f_{1m}(z)\,\mathrm{d}z = \int_{-h_1}^{h_0} \phi_2(0,z) f_{1m}(z)\,\mathrm{d}z, \\ \displaystyle\int_{-h_2}^{h_0} \phi_{1x}(0,z) f_{2m}(z)\, H(z+h_1)\,\mathrm{d}z = \int_{-h_2}^{h_0} \phi_{2x}(0,z) f_{2m}(z)\,\mathrm{d}z. \end{cases} \tag{A2}$$

Using (4.1) and (4.4), and taking into account the Heaviside functions that shift the limits of integration, (A1) is rewritten as

$$
\frac{\mathrm{i}}{k_{10}}(1 + R_0)\left[\int_{-h_2}^{0} \frac{\cosh k_{10}(z + h_1)\cosh k_{2m}(z + h_2)}{\sinh k_{10}h_1 \sinh k_{2m}h_2}\,\mathrm{d}z\right.
$$

$$
\left. + \int_{0}^{h_0} \frac{\cosh k_{10}(z - h_0)\cosh k_{2m}(z - h_0)}{\sinh k_{10}h_0 \sinh k_{2m}h_0}\,\mathrm{d}z\right]
$$

$$
+ \sum_{n=1}^{\infty} \frac{1}{k_{1n}} R_n \left[\int_{-h_2}^{0} \frac{\cosh k_{1n}(z + h_1)\cosh k_{2m}(z + h_2)}{\sinh k_{1n}h_1 \sinh k_{2m}h_2}\,\mathrm{d}z\right.
$$

$$
\left. + \int_{0}^{h_0} \frac{\cosh k_{1n}(z - h_0)\cosh k_{2m}(z - h_0)}{\sinh k_{1n}h_0 \sinh k_{2m}h_0}\,\mathrm{d}z\right]
$$

$$
= \frac{\mathrm{i}}{k_{20}} T_0 \left[\int_{-h_2}^{0} \frac{\cosh k_{20}(z + h_2)\cosh k_{2m}(z + h_2)}{\sinh k_{20}h_2 \sinh k_{2m}h_2}\,\mathrm{d}z\right.
$$

$$
\left. + \int_{0}^{h_0} \frac{\cosh k_{20}(z - h_0)\cosh k_{2m}(z - h_0)}{\sinh k_{20}h_0 \sinh k_{2m}h_0}\,\mathrm{d}z\right]
$$

$$
+ \sum_{n=1}^{\infty} \frac{1}{k_{2n}} T_n \left[\int_{-h_2}^{0} \frac{\cosh k_{2n}(z + h_2)\cosh k_{2m}(z + h_2)}{\sinh k_{2n}h_2 \sinh k_{2m}h_2}\,\mathrm{d}z\right.
$$

$$
\left. + \int_{0}^{h_0} \frac{\cosh k_{2n}(z - h_0)\cosh k_{2m}(z - h_0)}{\sinh k_{2n}h_0 \sinh k_{2m}h_0}\,\mathrm{d}z\right] \tag{A3}
$$

and

$$
- (1 - R_0)\left[\int_{-h_1}^{0} \frac{\cosh k_{10}(z + h_1)\cosh k_{1m}(z + h_1)}{\sinh k_{10}h_1 \sinh k_{1m}h_1}\,\mathrm{d}z\right.
$$

$$
\left. + \int_{0}^{h_0} \frac{\cosh k_{10}(z - h_0)\cosh k_{1m}(z - h_0)}{\sinh k_{10}h_0 \sinh k_{1m}h_0}\,\mathrm{d}z\right]
$$

$$
+ \sum_{n=1}^{\infty} R_n \left[\int_{-h_1}^{0} \frac{\cosh k_{1n}(z + h_1)\cosh k_{1m}(z + h_1)}{\sinh k_{1n}h_1 \sinh k_{1m}h_1}\,\mathrm{d}z\right.
$$

$$
\left. + \int_{0}^{h_0} \frac{\cosh k_{1n}(z - h_0)\cosh k_{1m}(z - h_0)}{\sinh k_{1n}h_0 \sinh k_{1m}h_0}\,\mathrm{d}z\right]
$$

$$
= -T_0 \left[\int_{-h_2}^{0} \frac{\cosh k_{20}(z + h_2)\cosh k_{1m}(z + h_1)}{\sinh k_{20}h_2 \sinh k_{1m}h_1}\,\mathrm{d}z\right.
$$

$$
\left. + \int_{0}^{h_0} \frac{\cosh k_{20}(z - h_0)\cosh k_{1m}(z - h_0)}{\sinh k_{20}h_0 \sinh k_{1m}h_0}\,\mathrm{d}z\right]
$$

$$
- \sum_{n=1}^{\infty} T_n \left[\int_{-h_2}^{0} \frac{\cosh k_{2n}(z + h_2) \cosh k_{1m}(z + h_1)}{\sinh k_{2n}h_2 \sinh k_{1m}h_1} \, \mathrm{d}z \right.
$$

$$
\left. + \int_{0}^{h_0} \frac{\cosh k_{2n}(z - h_0) \cosh k_{1m}(z - h_0)}{\sinh k_{2n}h_0 \sinh k_{1m}h_0} \, \mathrm{d}z \right]. \tag{A4}
$$

Similarly, using (4.1) and (4.4), (A2) can be rewritten as

$$
\frac{\mathrm{i}}{k_{10}} (1 + R_0) \left[\int_{-h_1}^{0} \frac{\cosh k_{10}(z + h_1) \cosh k_{1m}(z + h_1)}{\sinh k_{10}h_1 \sinh k_{1m}h_1} \, \mathrm{d}z \right.
$$

$$
\left. + \int_{0}^{h_0} \frac{\cosh k_{10}(z - h_0) \cosh k_{1m}(z - h_0)}{\sinh k_{10}h_0 \sinh k_{1m}h_0} \, \mathrm{d}z \right]
$$

$$
+ \sum_{n=1}^{\infty} \frac{1}{k_{1n}} R_n \left[\int_{-h_1}^{0} \frac{\cosh k_{1n}(z + h_1) \cosh k_{1m}(z + h_1)}{\sinh k_{1n}h_1 \sinh k_{1m}h_1} \, \mathrm{d}z \right.
$$

$$
\left. + \int_{0}^{h_0} \frac{\cosh k_{1n}(z - h_0) \cosh k_{1m}(z - h_0)}{\sinh k_{1n}h_0 \sinh k_{1m}h_0} \, \mathrm{d}z \right]
$$

$$
= \frac{\mathrm{i}}{k_{20}} T_0 \left[\int_{-h_1}^{0} \frac{\cosh k_{20}(z + h_2) \cosh k_{1m}(z + h_1)}{\sinh k_{20}h_2 \sinh k_{1m}h_1} \, \mathrm{d}z \right.
$$

$$
\left. + \int_{0}^{h_0} \frac{\cosh k_{20}(z - h_0) \cosh k_{1m}(z - h_0)}{\sinh k_{20}h_0 \sinh k_{1m}h_0} \, \mathrm{d}z \right]
$$

$$
+ \sum_{n=1}^{\infty} \frac{1}{k_{2n}} T_n \left[\int_{-h_1}^{0} \frac{\cosh k_{2n}(z + h_2) \cosh k_{1m}(z + h_1)}{\sinh k_{2n}h_2 \sinh k_{1m}h_1} \, \mathrm{d}z \right.
$$

$$
\left. + \int_{0}^{h_0} \frac{\cosh k_{2n}(z - h_0) \cosh k_{1m}(z - h_0)}{\sinh k_{2n}h_0 \sinh k_{1m}h_0} \, \mathrm{d}z \right] \tag{A5}
$$

and

$$
- (1 - R_0) \left[\int_{-h_1}^{0} \frac{\cosh k_{10}(z + h_1) \cosh k_{2m}(z + h_2)}{\sinh k_{10}h_1 \sinh k_{2m}h_2} \, \mathrm{d}z \right.
$$

$$
\left. + \int_{0}^{h_0} \frac{\cosh k_{10}(z - h_0) \cosh k_{2m}(z - h_0)}{\sinh k_{10}h_0 \sinh k_{2m}h_0} \, \mathrm{d}z \right]
$$

$$
+ \sum_{n=1}^{\infty} R_n \left[\int_{-h_1}^{0} \frac{\cosh k_{1n}(z + h_1) \cosh k_{2m}(z + h_2)}{\sinh k_{1n}h_1 \sinh k_{2m}h_2} \, \mathrm{d}z \right.
$$

$$
\left. + \int_{0}^{h_0} \frac{\cosh k_{1n}(z - h_0) \cosh k_{2m}(z - h_0)}{\sinh k_{1n}h_0 \sinh k_{2m}h_0} \, \mathrm{d}z \right]
$$

$$= -T_0 \left[\int_{-h_2}^{0} \frac{\cosh k_{20}(z + h_2) \cosh k_{2m}(z + h_2)}{\sinh k_{20}h_2 \sinh k_{2m}h_2} \, dz \right.$$

$$+ \left. \int_{0}^{h_0} \frac{\cosh k_{20}(z - h_0) \cosh k_{2m}(z - h_0)}{\sinh k_{20}h_0 \sinh k_{2m}h_0} \, dz \right]$$

$$- \sum_{n=1}^{\infty} T_n \left[\int_{-h_2}^{0} \frac{\cosh k_{2n}(z + h_2) \cosh k_{2m}(z + h_2)}{\sinh k_{2n}h_2 \sinh k_{2m}h_2} \, dz \right.$$

$$+ \left. \int_{0}^{h_0} \frac{\cosh k_{2n}(z - h_0) \cosh k_{2m}(z - h_0)}{\sinh k_{2n}h_0 \sinh k_{2m}h_0} dz \right]. \tag{A6}$$

Then, it is required to calculate the following integrals:

$$\left. \begin{aligned}
a_{k_{1n}k_{2m}}^{1)} &= \int_{0}^{h_0} \frac{\cosh k_{1n}(z - h_0) \cosh k_{2m}(z - h_0)}{\sinh k_{1n}h_0 \sinh k_{2m}h_0} \, dz, \\
a_{k_{2n}k_{2m}}^{2)} &= \int_{0}^{h_0} \frac{\cosh k_{2n}(z - h_0) \cosh k_{2m}(z - h_0)}{\sinh k_{2n}h_0 \sinh k_{2m}h_0} \, dz, \\
a_{k_{1n}k_{1m}}^{3)} &= \int_{0}^{h_0} \frac{\cosh k_{1n}(z - h_0) \cosh k_{1m}(z - h_0)}{\sinh k_{1n}h_0 \sinh k_{1m}h_0} \, dz, \\
a_{k_{2n}k_{1m}}^{4)} &= \int_{0}^{h_0} \frac{\cosh k_{2n}(z - h_0) \cosh k_{1m}(z - h_0)}{\sinh k_{2n}h_0 \sinh k_{1m}h_0} \, dz, \\
b_{k_{1n}k_{2m}}^{1)} &= \int_{-h_2}^{0} \frac{\cosh k_{1n}(z + h_1) \cosh k_{2m}(z + h_2)}{\sinh k_{1n}h_1 \sinh k_{2m}h_2} \, dz, \\
b_{k_{2n}k_{2m}}^{2)} &= \int_{-h_2}^{0} \frac{\cosh k_{2n}(z + h_2) \cosh k_{2m}(z + h_2)}{\sinh k_{2n}h_2 \sinh k_{2m}h_2} \, dz, \\
b_{k_{1n}k_{1m}}^{3)} &= \int_{-h_1}^{0} \frac{\cosh k_{1n}(z + h_1) \cosh k_{1m}(z + h_1)}{\sinh k_{1n}h_1 \sinh k_{1m}h_1} \, dz, \\
b_{k_{2n}k_{1m}}^{4)} &= \int_{-h_1}^{0} \frac{\cosh k_{2n}(z + h_2) \cosh k_{1m}(z + h_1)}{\sinh k_{2n}h_2 \sinh k_{1m}h_1} \, dz.
\end{aligned} \right\} \tag{A7}$$

In short, we need to calculate three types of integrals:

$$a_{\alpha_n \beta_m}^{1)-4)} = \int_{0}^{h} \frac{\cosh \alpha_n(z - h) \cosh \beta_m(z - h)}{\sinh \alpha_n h \sinh \beta_m h} \, dz, \tag{A8}$$

$$b_{\alpha_n \beta_m}^{1),4)} = \int_{-h}^{0} \frac{\cosh \alpha_n(z + d) \cosh \beta_m(z + h)}{\sinh \alpha_n d \sinh \beta_m h} \, dz, \tag{A9}$$

$$b_{\beta_n \beta_m}^{2),3)} = \int_{-h}^{0} \frac{\cosh \beta_n(z + h) \cosh \beta_m(z + h)}{\sinh \beta_n h \sinh \beta_m h} \, dz. \tag{A10}$$

Here, h is an arbitrary constant, which may be either h_0, or h_1 or h_2. Note that d is also an arbitrary constant such that $d \neq h$. For example, if $h = h_1$, then $d = h_2$, and *vice versa*.

Consequently, (A3) and (A4) in the case $h_1 \geq h_2$ reduce to the form

$$
\begin{cases}
\dfrac{\mathrm{i}R_0}{k_{10}} \left[b^{1)}_{k_{10}k_{2m}} + a^{1)}_{k_{10}k_{2m}} \right] + \displaystyle\sum_{n=1}^{\infty} \dfrac{R_n}{k_{1n}} \left[b^{1)}_{k_{1n}k_{2m}} + a^{1)}_{k_{1n}k_{2m}} \right] - \dfrac{\mathrm{i}T_0}{k_{20}} \left[b^{2)}_{k_{20}k_{2m}} + a^{2)}_{k_{20}k_{2m}} \right] \\[3mm]
\quad - \displaystyle\sum_{n=1}^{\infty} \dfrac{T_n}{k_{2n}} \left[b^{2)}_{k_{2n}k_{2m}} + a^{2)}_{k_{2n}k_{2m}} \right] = -\dfrac{\mathrm{i}}{k_{10}} \left[b^{1)}_{k_{10}k_{2m}} + a^{1)}_{k_{10}k_{2m}} \right], \\[3mm]
-R_0 \left[b^{3)}_{k_{10}k_{1m}} + a^{3)}_{k_{10}k_{1m}} \right] - \displaystyle\sum_{n=1}^{\infty} R_n \left[b^{3)}_{k_{1n}k_{1m}} + a^{3)}_{k_{1n}k_{1m}} \right] \\[3mm]
\quad - T_0 \left[b^{4)}_{k_{20}k_{1m}} H(z+h_2) + a^{4)}_{k_{20}k_{1m}} \right] - \displaystyle\sum_{n=1}^{\infty} T_n \left[b^{4)}_{k_{2n}k_{1m}} H(z+h_2) + a^{4)}_{k_{2n}k_{1m}} \right] \\[3mm]
\quad = -\left[b^{3)}_{k_{10}k_{1m}} + a^{3)}_{k_{10}k_{1m}} \right].
\end{cases}
\tag{A11}
$$

Proceeding similarly, (A5) and (A6) for $h_1 \leq h_2$ reduce to

$$
\begin{cases}
\dfrac{\mathrm{i}R_0}{k_{10}} \left[b^{3)}_{k_{10}k_{1m}} + a^{3)}_{k_{10}k_{1m}} \right] + \displaystyle\sum_{n=1}^{\infty} \dfrac{R_n}{k_{1n}} \left[b^{3)}_{k_{1n}k_{1m}} + a^{3)}_{k_{1n}k_{1m}} \right] - \dfrac{\mathrm{i}T_0}{k_{20}} \left[b^{4)}_{k_{20}k_{1m}} + a^{4)}_{k_{20}k_{1m}} \right] \\[3mm]
\quad - \displaystyle\sum_{n=1}^{\infty} \dfrac{T_n}{k_{2n}} \left[b^{4)}_{k_{2n}k_{1m}} + a^{4)}_{k_{2n}k_{1m}} \right] = -\dfrac{\mathrm{i}}{k_{10}} \left[b^{3)}_{k_{10}k_{1m}} + a^{3)}_{k_{10}k_{1m}} \right], \\[3mm]
-R_0 \left[b^{1)}_{k_{10}k_{2m}} H(z+h_1) + a^{1)}_{k_{10}k_{2m}} \right] - \displaystyle\sum_{n=1}^{\infty} R_n \left[b^{1)}_{k_{1n}k_{2m}} H(z+h_1) + a^{1)}_{k_{1n}k_{2m}} \right] \\[3mm]
\quad - T_0 \left[b^{2)}_{k_{20}k_{2m}} + a^{2)}_{k_{20}k_{2m}} \right] - \displaystyle\sum_{n=1}^{\infty} T_n \left[b^{2)}_{k_{2n}k_{2m}} + a^{2)}_{k_{2n}k_{2m}} \right] \\[3mm]
\quad = -\left[b^{1)}_{k_{10}k_{2m}} H(z+h_1) + a^{1)}_{k_{10}k_{2m}} \right].
\end{cases}
\tag{A12}
$$

Here, the integrals $a^{1)-4)}_{\alpha_n \beta_m}$, $b^{1),4)}_{\alpha_n \beta_m}$ and $b^{2),3)}_{\beta_n \beta_m}$ are evaluated as

$$
\begin{aligned}
a^{1)-4)}_{\alpha_n \beta_m} &= \int_0^h \frac{\cosh \alpha_n(z-h) \cosh \beta_m(z-h)}{\sinh \alpha_n h \, \sinh \beta_m h} \, \mathrm{d}z \\
&= \begin{cases}
\dfrac{\alpha_n \coth \beta_m h - \beta_m \coth \alpha_n h}{\alpha_n^2 - \beta_m^2} & \text{for } \alpha_n \neq \beta_m, \\[3mm]
\dfrac{\mathrm{e}^{4\alpha_n h} + 4\alpha_n h \, \mathrm{e}^{2\alpha_n h} - 1}{2\alpha_n (1 - \mathrm{e}^{2\alpha_n h})^2} & \text{for } \alpha_n = \beta_m,
\end{cases}
\end{aligned}
\tag{A13}
$$

$$
\begin{aligned}
b^{1),4)}_{\alpha_n \beta_m} &= \int_{-h}^0 \frac{\cosh \alpha_n(z+d) \cosh \beta_m(z+h)}{\sinh \alpha_n d \, \sinh \beta_m h} \, \mathrm{d}z, \\
&= \begin{cases}
\dfrac{\alpha_n \{\sinh \alpha_n(h-d) + \cosh \beta_m h \sinh \alpha_n d\} + \beta_m \sinh \beta_m h \cosh \alpha_n d}{\sinh \beta_m h \, \sinh \alpha_n d \, (\alpha_n^2 - \beta_m^2)} & \text{for } \alpha_n \neq \beta_m, \\[3mm]
\dfrac{\coth \alpha_n d\{1 + h\alpha_n \coth \alpha_n h\} - \alpha_n h}{2\alpha_n} & \text{for } \alpha_n = \beta_m,
\end{cases}
\end{aligned}
\tag{A14}
$$

$$b_{\beta_n\beta_m}^{2),3)} = \int_{-h}^{0} \frac{\cosh\beta_n(z+h)\cosh\beta_m(z+h)}{\sinh\beta_n h \sinh\beta_m h}\,\mathrm{d}z,$$

$$= \begin{cases} \dfrac{\beta_n \coth\beta_m h - \beta_m \coth\beta_n h}{(\beta_n^2 - \beta_m^2)} & \text{for } \beta_m \neq \beta_n, \\[2mm] \dfrac{\mathrm{e}^{4\beta_n h} + 4\beta_n h\,\mathrm{e}^{2\beta_n h} - 1}{2\beta_n(1 - \mathrm{e}^{2\beta_n h})^2} & \text{for } \beta_n = \beta_m. \end{cases} \tag{A15}$$

It is important to emphasize that when dealing with gravitational waves at the interface between two layers of arbitrary density, the eigenfunctions f_{jm}, $j = 1, 2$, associated with the set of propagating and evanescent wave modes defined by the dispersion relation (3.2) are generally non-orthogonal. However, if we restrict our analysis to fluids with almost the same densities (in the Boussinesq approximation; Brekhovskikh & Goncharov 1994), then the eigenfunctions become orthogonal, and the corresponding dispersion relation (3.2) reduces to

$$\omega^2 = \frac{g' k_j}{a \coth k_j h_0 + \coth k_j h_j}, \tag{A16}$$

where $g' = (1 - a)g$ is the reduced acceleration due to gravity. In this case, the following relationship holds:

$$\alpha_n \coth\beta_m h_0 - \beta_m \coth\alpha_n h_0 + \alpha_n \coth\beta_m h_1 - \beta_m \coth\alpha_n h_1$$
$$= \alpha_n(\coth\beta_m h_0 + \coth\beta_m h_1) - \beta_m(\coth\alpha_n h_0 + \coth\alpha_n h_1)$$
$$= \alpha_n\beta_m g'/\omega^2 - \beta_m\alpha_n g'/\omega^2 = 0. \tag{A17}$$

This leads to the identity $a_{\beta_n\beta_m}^{1)-4)} + b_{\beta_n\beta_m}^{2),3)} = 0$ for $n \neq m$. However, for the sake of generality, such a simplification will not be used in further calculations.

Next, we evaluate integrals in (A11):

$$a_{k_{1n}k_{2m}}^{1)} + b_{k_{1n}k_{2m}}^{1)}$$

$$= \begin{cases} \dfrac{\begin{aligned}&k_{1n}\{\sinh k_{1n}(h_1 - h_2) - \cosh k_{2m}h_2 \sinh k_{1n}h_1\} \\ &\quad + k_{2m}\cosh k_{1n}h_1 \sinh k_{2m}h_2\end{aligned}}{\sinh k_{1n}h_1 \sinh k_{2m}h_2(k_{2m}^2 - k_{1n}^2)} \\[4mm] \quad - \dfrac{k_{1n}\coth k_{2m}h_0}{k_{2m}^2 - k_{1n}^2} + \dfrac{k_{1n}k_{2m}\cosh k_{2m}h_0 \coth k_{1n}h_0}{k_{2m}^2 - k_{1n}^2} & \text{for } k_{1n} \neq k_{2m}, \\[4mm] \dfrac{\mathrm{e}^{4k_{1n}h_0} + 4k_{1n}h_0\,\mathrm{e}^{2k_{1n}h_0} - 1}{2k_{1n}(1 - \mathrm{e}^{2k_{1n}h_0})^2} \\[4mm] \quad + \dfrac{\coth k_{1n}h_1\{1 + k_{1n}h_2\coth k_{1n}h_2\} - k_{1n}h_2}{2k_{1n}} & \text{for } k_{1n} = k_{2m}, \end{cases} \tag{A18}$$

$$a^{2)}_{k_{2n}k_{2m}} + b^{2)}_{k_{2n}k_{2m}}$$

$$= \begin{cases} \dfrac{k_{2m}\coth k_{2n}h_0}{k_{2m}^2 - k_{1n}^2} - \dfrac{k_{2n}\coth k_{2m}h_2}{k_{2m}^2 - k_{2n}^2} - \dfrac{k_{2n}\coth k_{2m}h_0}{k_{2m}^2 - k_{1n}^2} + \dfrac{k_{2m}\coth k_{2n}h_2}{k_{2m}^2 - k_{2n}^2} & \text{for } m \neq n, \\[4mm] \dfrac{e^{4h_0 k_{2m}} + 4k_{2m}h_0\, e^{2k_{2m}h_0} - 1}{2k_{2m}(e^{2k_{2m}h_0} - 1)^2} + \dfrac{e^{4h_2 k_{2m}} + 4k_{2m}h_2\, e^{2h_2 k_{2m}} - 1}{2k_{2m}(e^{2k_{2m}h_2} - 1)^2} & \text{for } m = n, \end{cases}$$

$$\text{(A19)}$$

$$a^{3)}_{k_{1n}k_{1m}} + b^{3)}_{k_{1n}k_{1m}}$$

$$= \begin{cases} \dfrac{k_{1m}(\coth k_{1n}h_0 - \coth k_{1n}h_1) - k_{1n}(\coth k_{1m}h_1 + \coth k_{1m}h_0)}{k_{1m}^2 - k_{1n}^2} & \text{for } m \neq n, \\[4mm] \dfrac{e^{4k_{1n}h_0} + 4k_{1n}h_0\, e^{2k_{1n}h_0} - 1}{2k_{1n}(e^{2k_{1n}h_0} - 1)^2} + \dfrac{e^{4k_{1n}h_1} + 4k_{1n}h_1\, e^{2k_{1n}h_1} - 1}{2k_{1n}(e^{2k_{1n}h_1} - 1)^2} & \text{for } m = n, \end{cases}$$

$$\text{(A20)}$$

$$a^{4)}_{k_{2n}k_{1m}} H(z + h_2) + b^{4)}_{k_{2n}k_{1m}}$$

$$= \begin{cases} -\dfrac{k_{1m}\{\sinh k_{1m}(h_1 - h_2) - \cosh k_{2n}h_2 \sinh k_{1m}h_1\} + k_{2n}\cosh k_{1m}h_1 \sinh k_{2n}h_2}{\sinh k_{1m}h_1 \sinh k_{2n}h_2\,(k_{1m}^2 - k_{2n}^2)} \\[4mm] \quad + \dfrac{k_{1m}\coth k_{2n}h_0 - k_{2n}\coth k_{1m}h_0}{k_{1m}^2 - k_{2n}^2} \qquad\qquad \text{for } k_{1m} \neq k_{2n}, \\[4mm] \dfrac{e^{4k_{2n}h_0} + 4k_{2n}h_0\, e^{2k_{2n}h_0} - 1}{2k_{2n}(1 - e^{2k_{2n}h_0})^2} - \dfrac{h_2}{2} \\[4mm] \quad + \dfrac{\cosh k_{2n}h_1\,\{\sinh k_{2n}h_2 + k_{2n}h_2\cosh k_{2n}h_2\}}{2k_{2n}\sinh k_{2n}h_1 \sinh k_{2n}h_2} \quad \text{for } k_{1n} = k_{2m}. \end{cases}$$

$$\text{(A21)}$$

Subsequently, by solving a finite system of linear equations as in each of (A11) and (A12) for a finite number of sum terms, say N, the unknowns R_n and T_n can be determined. It is pertinent to note that the reflection and transmission coefficients K_r and K_t are defined as $K_r = |R_n|$ and $K_t = |T_n|$.

It can be easily verified that the reflection coefficient K_r and the transmission coefficient K_t satisfy the energy balance relation

$$F \equiv K_r^2 + \chi K_t^2 = 1, \tag{A22}$$

where $\chi = c_g(k_t)/c_g(k_i)$ is the ratio of group speeds of transmitted and incident waves.

REFERENCES

BARTHOLOMEUSZ, L. 1958 The reflection of long waves at a step. *Math. Proc. Camb. Phil. Soc.* **54**, 106–118.

BREKHOVSKIKH, L.M. & GONCHAROV, V.V. 1994 *Mechanics of Continua and Wave Dynamics*. Springer.

CHURAEV, E.N., SEMIN, S.V. & STEPANYANTS, Y.A. 2015 Transformation of internal waves passing over a bottom step. *J. Fluid Mech.* **368**, R3.

CHURILOV, S.M. & STEPANYANTS, Y.A. 2022a Reflectionless wave propagation on shallow water with variable bathymetry and current. *J. Fluid Mech.* **931**, A15.

CHURILOV, S.M. & STEPANYANTS, Y.A. 2022b Reflectionless wave propagation on shallow water with variable bathymetry and current. Part 2. *J. Fluid Mech.* **939**, A15.

DINGEMANS, M.W. 1997 *Water Wave Propagation Over Uneven Bottoms*. World Scientific.

DUCROZET, G., SLUNYAEV, A.V. & STEPANYANTS, Y.A. 2021 Transformation of envelope solitons on a bottom step. *Phys. Fluids* **33**, 066606.

GINIYATULLIN, A., KURKIN, A., SEMIN, S. & STEPANYANTS, Y. 2014 Transformation of narrowband wavetrains of surface gravity waves passing over a bottom step. *Math. Model. Nat. Phenom.* **9**, 73–82.

GRIMSHAW, R., PELINOVSKY, E. & TALIPOVA, T. 2008 Fission of a weakly nonlinear interfacial solitary wave at a step. *Geophys. Astro. Fluid* **102**, 179–194.

KURKIN, A., SEMIN, S. & STEPANYANTS, Y. 2015 Surface water waves transformation over a bottom ledge. *Izv. Atmos. Ocean. Phys.* **50**, 29–35.

LAMB, H. 1932 *Hydrodynamics*, 6th edn. Cambridge University Press.

MADERICH, V., TALIPOVA, T., GRIMSHAW, R., PELINOVSKY, E., CHOI, B., BROVCHENKO, I., TERLETSKA, K. & KIM, D. 2009 The transformation of interfacial solitary wave of elevation at a bottom step. *Nonlinear Process. Geophys.* **16**, 33–42.

MADERICH, V., TALIPOVA, T., GRIMSHAW, R., TERLETSKA, K., BROVCHENKO, I., PELINOVSKY, E. & BYUNG, H. 2010 Interaction of a large amplitude interfacial solitary wave of depression with bottom step. *Phys. Fluids* **22**, 1–12.

MASSEL, S.R. 1989 *Hydrodynamics of the Coastal Zone*. Elsevier.

MEYLAN, M.H. & STEPANYANTS, Y.A. 2024 Scattering of gravity-capillary waves on a bottom step. *Phys. Fluids* **36**, 017104.

MILES, J. 1967 Surface-wave scattering matrix for a shelf. *J. Fluid Mech.* **28**, 755–767.

MIROPOL'SKY, Y.Z. 2001 *Dynamics of Internal Gravity Waves in the Ocean*. Springer Science & Business Media.

TAKANO, K. 1960 Effets d'un obstacle parallelepipedique sur la propagation de la houle. *La Houille Blanche* **15**, 247–267.

TAKANO, K. 1967 Effet d'un changement brusque de profondeur sur une houle irrotationelle. *La Mer* **5** (2), 100–116.